

■ **BIOMATERIALS**

In vivo cartilage regeneration in a multi-layered articular cartilage architecture mimicking scaffold

**K. Rajagopal,
S. Ramesh,
N. M. Walter,
A. Arora,
D. S. Katti,
V. Madhuri**

*From Christian Medical
College, Vellore, India*

Aims

Extracellular matrix (ECM) and its architecture have a vital role in articular cartilage (AC) structure and function. We hypothesized that a multi-layered chitosan-gelatin (CG) scaffold that resembles ECM, as well as native collagen architecture of AC, will achieve superior chondrogenesis and AC regeneration. We also compared its in vitro and in vivo outcomes with randomly aligned CG scaffold.

Methods

Rabbit bone marrow mesenchymal stem cells (MSCs) were differentiated into the chondrogenic lineage on scaffolds. Quality of in vitro regenerated cartilage was assessed by cell viability, growth, matrix synthesis, and differentiation. Bilateral osteochondral defects were created in 15 four-month-old male New Zealand white rabbits and segregated into three treatment groups with five in each. The groups were: 1) untreated and allogeneic chondrocytes; 2) multi-layered scaffold with and without cells; and 3) randomly aligned scaffold with and without cells. After four months of follow-up, the outcome was assessed using histology and immunostaining.

Results

In vitro testing showed that the secreted ECM oriented itself along the fibre in multi-layered scaffolds. Both types of CG scaffolds supported cell viability, growth, and matrix synthesis. In vitro chondrogenesis on scaffold showed an around 400-fold increase in collagen type 2 (COL2A1) expression in both CG scaffolds, but the total glycosaminoglycan (GAG)/DNA deposition was 1.39-fold higher in the multi-layered scaffold than the randomly aligned scaffold. In vivo cartilage formation occurred in both multi-layered and randomly aligned scaffolds treated with and without cells, and was shown to be of hyaline phenotype on immunostaining. The defects treated with multi-layered + cells, however, showed significantly thicker cartilage formation than the randomly aligned scaffold.

Conclusion

We demonstrated that MSCs loaded CG scaffold with multi-layered zonal architecture promoted superior hyaline AC regeneration.

Cite this article: *Bone Joint Res* 2020;9(9):601–612.

Keywords: Articular cartilage, Mesenchymal stem cell, Multi-layered scaffold, Chondrogenic differentiation, Rabbit osteochondral model.

Article focus

- This study tested the role of multi-layered articular cartilage (AC) structure mimicking scaffold (with aligned fibres) in hyaline AC regeneration.
- Regeneration potential of the multi-layered scaffold was tested in the rabbit osteochondral defect model and the outcome was compared with the defects treated with randomly aligned scaffold.

Key messages

- Both types of chitosan-gelatin (CG) scaffolds (multi-layered and randomly aligned scaffold) promoted chondrogenesis of mesenchymal stem cells (MSCs) in vitro
- Multi-layered scaffold supported higher glycosaminoglycan (GAG) deposition than the randomly aligned scaffold in vitro.

Correspondence should be sent to
Dr Vrisha Madhuri; email:
madhuriwalter@cmcvellore.ac.in

doi: 10.1302/2046-3758.99.BJR-
2019-0210.R2

Bone Joint Res 2020;9(9):601–612.

- Multi-layered scaffold facilitated the AC repair and showed thicker hyaline cartilage formation in vivo than the randomly aligned scaffold.

Strengths and limitations

- This study is the first to report the in vivo regeneration potential of the multi-layered AC zonal architecture mimicking scaffold.
- A longer follow-up and tracking of transplanted cells could have strengthened our findings.

Introduction

Articular cartilage (AC) is composed of extracellular matrix (ECM) and cells, with chondrocytes accounting for about 1% to 10% of the total tissue. It has minimal self-healing ability due to its sparse population of progenitor cells and its avascular nature (which impedes the recruitment of adjacent stem/progenitor cells). Eventually, the healing of injured AC requires exogenous support.^{1,2}

Clinically, two strategies have commonly been used for restoration of damaged cartilage. The first is autologous chondrocyte transplantation (ACT) and the second is the release of subadjacent bone marrow stem cells by microfracture.³ Both methods have achieved cartilage repair and demonstrated short-term improvement in knee function and pain relief.³ Nevertheless, in the long term this outcome has not been sustained because of mechanically inferior fibrocartilage formation in the damaged area.^{4,5} Furthermore, the limitations of ACT include lack of proliferative capacity of chondrocytes in older patients, dedifferentiation of chondrocytes during expansion, and donor site morbidity, which necessitate finding an alternative treatment option.⁶ Current strategy involves the use of scaffolds to provide the 3D environment, cartilage niche, and the ability to withstand compressive and shear stress during weight-bearing and articulation to stimulate optimal AC repair.

Natural materials are often considered as scaffolds for cartilage regeneration because they mimic physiological structure and provide an adhesion surface and a natural niche for regenerating cells. They are biocompatible, biodegradable, and their degradation products are not toxic. Chitosan, a deacetylated form of chitin, mimics the structure of the glycosaminoglycan (GAG) in AC.⁷ Gelatin, a denatured product derived from collagen, favours cell attachment because of the presence of Arg–Gly–Asp peptides.⁸ Chitosan-gelatin (CG) scaffolds have in the past been used for AC repair, but success has been limited by their poor mechanical performance.⁹

AC is organized into three distinct zones: superficial, middle, and deep. In the superficial zone, collagen fibrils are densely packed and arranged parallel to the articular surface, a configuration that resists shear stress generated during movement. In the middle zone, fibrils are oriented in a random fashion, helping to resist initial compression, while in the deep zone fibrils are perpendicular to the

surface, providing further compressive strength to the AC.² Therefore, an ideal scaffold suitable for cartilage tissue engineering should possibly have structural organization similar to the native AC.^{10,11} One of the authors (DSK) has previously fabricated multi-layered scaffolds (pore size 160 μm) and demonstrated the renderings of the collagen fibre orientation on the superficial and transition zones using scanning electron microscope (SEM) and fluorescence imaging techniques¹¹, while randomly aligned scaffolds had a mean pore size of 283 μm . Mechanical testing also revealed that the compressive modulus of the multi-layered scaffold (7 kPa) was higher than the randomly aligned scaffold (3 kPa).¹¹ Although previous in vitro studies have attempted to highlight the importance of collagen fibre orientation on scaffolds,^{10,11} this strategy has not been tested in in vivo animal models of AC injury.

In this study we have used a multi-layered CG scaffold, which mimics the orientation of collagen fibres on the superficial and transition zones as well as the ECM components of AC. We hypothesized that such a scaffold would improve cartilage repair by facilitating chondrogenesis from mesenchymal stem cells (MSCs) and provide a greater mechanical strength. The comparison group used was a CG scaffold without such a zonal arrangement. Initial in vitro studies were followed by in vivo experiments to assess the suitability of multi-layered CG scaffolds for cartilage repair.

Methods

The study protocol was approved by the institutional review board and the institutional animal ethics committee of Christian Medical College, Vellore, India. The experiments were conducted in accordance with the national guidelines for experimentation on animals and in an approved animal facility.

Isolation and characterization of bone marrow MSCs. Bone marrow was aspirated from eight four-month-old male New Zealand white rabbits (weighing 2 kg to 2.5 kg). MSCs were harvested using the Ficoll-Paque method and cultured with MSC culture media containing α -minimum essential medium (α -MEM) (Sigma-Aldrich, St Louis, Missouri, USA) supplemented with 10% fetal bovine serum (FBS) (Thermo Fisher Scientific, Grand Island, New York, USA), 5 ng/ml fibroblast growth factor (FGF-2) (PeproTech, Rocky Hill, New Jersey, USA), 50 $\mu\text{g}/\text{ml}$ gentamicin (Thermo Fisher Scientific), and 2 $\mu\text{g}/\text{ml}$ amphotericin-B (Thermo Fisher Scientific). Cells were expanded until third passage and characterized by flow cytometry and multilineage differentiation assay.

Flow cytometry analysis and multilineage differentiation. The cell surface markers (positive markers: CD81 and CD44; negative markers: CD34, CD90, and Human Leukocyte Antigen-DR (HLA-DR)) for characterization of rabbit MSCs were selected based on previous publications.^{12,13} Third passaged cells (2×10^5) were incubated with fluorescent conjugated antibodies under dark

Table 1. Study groups, treatment plans, and numbers of animals used for in vivo study.

Serial number	Group	Right knee	Left knee	Number of animals
1.	1	Allogeneic chondrocyte transplantation (positive control)	Defect left untreated (negative control)	5
2.	2	Multi-layered scaffold seeded with cells	Multi-layered scaffold without cells	5
3.	3	Randomly aligned scaffold seeded with cells	Randomly aligned scaffold without cells	5

condition for 30 minutes at room temperature. After incubation, cells were washed with phosphate-buffered saline (PBS) and pelletized at 500 g for ten minutes and resuspended in 200 μ l of PBS for analysis. Non-specific mouse immunoglobulin G antibody (BD Biosciences, San Jose, California, USA) was used as isotype controls. Samples were acquired using Becton Dickinson (BD) FACS Calibur (BD Biosciences) and results were analyzed using BD Cell Quest software version 6.0. (BD Biosciences)

Multilineage differentiation assay was performed as described in the Supplementary Material.

Scaffolds. Two types of CG scaffolds were developed by our bioengineering collaborators. A multi-layered scaffold with three zones, each mimicking the orientation of collagen fibres in the superficial, middle, and deep AC zones, was fabricated by sequential unidirectional freezing method, while a randomly aligned scaffold that was used as a comparison had its fibres aligned without any orientation. Additionally, 4 mm diameter \times 3 mm height scaffolds were used for both in vitro and in vivo testing. The morphological characteristics, porosity, and mechanical properties of both multi-layered and randomly aligned scaffolds have already been tested and published.¹¹ The protocols for the preparation of multi-layered and randomly aligned scaffolds are provided in the Supplementary Material.

In vitro testing of scaffolds. The third passaged rabbit bone marrow MSCs (BM-MSCs) ($n = 3$) were used for in vitro testing. Prior to cell seeding, the scaffolds were primed with MSC culture media for 24 hours in a CO₂ incubator. Cells at passage 3 (1×10^6 cells/ml per scaffold) suspended in MSC culture media were immersed along with a scaffold in a microcentrifuge tube and placed in a MACSmix Tube rotator (Miltenyi Biotec, Bergisch Gladbach, Germany) at 20 rpm. After 12 hours, cell-seeded scaffolds were transferred to ultra-low attachment plate (Corning, New York, USA) and cultured either with MSC culture medium (for cytotoxicity assay) or chondrogenic differentiation medium (to induce chondrogenesis).

Chondrogenic differentiation on scaffolds. Cell-seeded scaffolds were differentiated into chondrogenic lineage using Dulbecco's Modified Eagle Medium (DMEM)-high glucose supplemented with dexamethasone (100 μ M), ascorbate-2-phosphate (40 μ g/ml), $1 \times$ insulin-transferrin-sodium selenite + 1 media supplement, L-proline (40 μ g/ml), and sodium pyruvate (1 mM). Components of chondrogenic differentiation medium were obtained from Sigma-Aldrich. During differentiation, samples were

collected on the seventh, 14th, 21st, and 28th days of differentiation and used for biochemical and gene expression analyses as well as histology.

Cell viability, proliferation, and matrix synthesis on scaffolds. Cell viability and distribution on the scaffolds were assessed by LIVE/DEAD Cell Viability kit (Invitrogen, Carlsbad, California, USA) as per the manufacturer's protocol. The stained constructs were placed at a sagittal plane and Z-stack images with a maximum depth of 300 μ m were acquired using a confocal microscope (Olympus FV1000, Tokyo, Japan). A total of 20 Z-stack images at 10 μ m to 15 μ m intervals were taken from each scaffold. A minimum of five images were taken from each of the two duplicate scaffolds. Tissue-engineered constructs (two technical replicates \times three biological replicates \times four timepoints = 24 scaffolds per group) were lyophilized for 24 hours and incubated with 100 mM phosphate buffer (pH 6.5) containing 125 μ g/ml papain for 18 hours at 60°C. The samples were centrifuged at 10,000 g for ten minutes and the supernatant used to quantitate DNA, GAG, and total collagen as per the manufacturer's or published protocol using Quant-iT PicoGreen dsDNA Assay Kit (Invitrogen), dimethyl methylene blue (DMMB) (Sigma-Aldrich),² and Sircol Collagen Assay (Biocolor, Belfast, UK), respectively.

Histology. Tissue-engineered constructs (two technical replicates \times three biological replicates = six scaffolds per group) were fixed in 4% paraformaldehyde and processed for routine paraffin embedding. A series of 5 μ m sections were taken from the surface at a 100 μ m interval between each section. A minimum four sections were stained with Safranin O/Fast Green (Sigma-Aldrich) to visualize sulfated glycosaminoglycan.

Gene expression analysis. Tissue-engineered constructs (two technical replicates \times three biological replicates = six scaffolds each group per timepoint) were homogenized with TRI reagent and the total RNA was isolated as per the manufacturer's protocol. Prime script RT kit (Takara, Shiga, Japan) was used for complementary DNA (cDNA) synthesis and the expression of collagen type 2 (COL2A1), collagen type 10 (COL10A1), and collagen type 1 (COL1A1) was quantitated using real-time polymerase chain reaction (PCR). The β 2-microglobulin gene was used as the housekeeping gene and fold change was calculated using the 2^{- $\Delta\Delta$ Ct} method.

In vivo study. The experimental design and protocols were approved by the institutional animal ethics committee, Christian Medical College, Vellore, India. Rabbits were procured from an approved breeder (Mahaveera

Enterprises, Hyderabad, India) and quarantined for a month prior to experimental procedures. Animals were individually housed with access to diet approved by national guidelines for experimentation on animals. A total of 15 four-month-old male New Zealand white rabbits were segregated into three groups with five animals per group (Table I). Group 1 contained control animals with allogeneic chondrocytes treated (positive control) and untreated (negative control) defects, group 2 contained multi-layered scaffold treated animals, and group 3 contained randomly aligned scaffold treated animals.

Isolation and cryopreservation of chondrocytes from AC. AC slices were harvested from the knee joint of five rabbits that were euthanized for in vitro study. Chondrocytes were recovered by collagenase type 2 (2 mg/ml) digestion (Worthington Biochemical Corporation, Lakewood, New Jersey, USA) for 22 hours at 37°C in a CO₂ incubator. Isolated cells were cryopreserved (70% DMEM/F12, 20% FBS, and 10% dimethyl sulfoxide) and stored in liquid nitrogen.

Prior to transplant, cryopreserved chondrocytes were revived and cultured (1×10^5 cells/well in six-well plate) in DMEM/F12 medium supplemented with 10% FBS, ascorbic acid (50 µg/ml), gentamicin (50 µg/ml), and amphotericin-B (2 µg/ml). Confluent cells were allowed to grow for two more days to form a cell sheet. The latter was pelletized and used for transplantation in the positive control animals (allogeneic chondrocytes only).

Preparation of tissue-engineered constructs for transplantation. Third passaged allogeneic rabbit BM-MSCs ($n = 5$ biological samples) were used for in vivo testing. The BM-MSCs were seeded on the scaffolds as mentioned above. Prior to transplant, the cell-seeded constructs were differentiated into the chondrogenic lineage for seven days.

Creation of focal AC defects and transplantation. Rabbits were anaesthetized using an intramuscular injection of ketamine (10 mg/kg; Troikaa Pharmaceuticals, Ahmedabad, India) and xylazine (2 mg/kg; Indian Immunologicals Ltd, Hyderabad, India). Animals were placed in a supine position on the operating table. The knee joints of both hind limbs were shaved and sterilized with 10% W/W povidone-iodine solution. A knee arthrotomy was performed using a medial parapatellar skin incision, and the patella was displaced laterally to expose the trochlear groove. Cylindrical osteochondral defects (4 mm wide × 3 mm deep), one in each distal femur, were created in the centre of the trochlear groove using a power drill at low speed with continuous irrigation. The integrity of the subchondral bone was breached as described by Khan et al.¹⁴ The defects were created in both hind limbs. In one limb, they were either filled with the cell-seeded construct (press-fit technique) or allogeneic chondrocytes, while the contralateral limb was treated with scaffold without cells or left untreated in group 1 (Table I). The wounds were closed in layers. Postoperatively, all animals received antibiotics and analgesics for four days. For rehabilitation, they were allowed to move freely in their cages

and for short periods in an adjoining play area. After four months of follow-up, the rabbits were euthanized and their knee joints harvested.

Gross appearance. The nature of regenerated tissue in the defect, its integration with adjacent tissue, and the percentage of defect repair were macroscopically evaluated. Harvested femoral condyles were also photographed, so that a record of their gross appearance was obtained.

Histology and scoring. The condyles were fixed in 10% buffered formalin followed by decalcification in three parts of 10% buffered formalin and one part of formic acid (Thermo Fisher Scientific India Pvt. Ltd, Mumbai, India). Sagittal cuts were made perpendicular to the surface from the area of the defect and processed for paraffin embedding. Then, 5 µm sections were prepared and stained with Safranin O (counterstained with Fast Green). An independent senior pathologist (NMW) blinded to the study groups examined the sections. A minimum of three representative sections were obtained from each specimen and the degree of cartilage regeneration in the defects was quantitated using the O'Driscoll score based on the following criteria: nature of the predominant tissue; structural characteristics; freedom from cellular changes of degeneration; and freedom from degenerative changes in adjacent cartilage (Supplementary Table i).¹⁵ The final score ranges from zero to 24 points. A score of 24 implies complete repair of defect akin to normal AC, while a score of zero indicates poor healing. Thus the higher the score, the better the cartilage repair.

Immunohistochemistry. The quality of the in vivo regenerated tissue was also assessed by immunostaining for collagen type 2 and collagen type 10 as per a previously published protocol.^{16,17} Three sections (at a minimum of 100 µm intervals) were taken from each specimen and processed for immunohistochemistry. Sections were incubated with primary mouse anti-collagen type 2 (II-II6B3, dilution 1:5; Developmental Studies Hybridoma Bank, Iowa City, Iowa, USA) or rabbit anti-collagen type 10 antibody (234196, dilution 1:250; Merck KGaA, Darmstadt, Germany). Primary antibodies were detected using horseradish peroxidase (HRP) conjugated secondary antibody. Visualization was performed using 3,3'-diaminobenzidine to identify the HRP-labelled antigen.

Thickness and percentage of collagen type 2 staining in regenerated cartilage were measured using ImageJ v1.52a software (National Institutes of Health, Bethesda, Maryland, USA).

Statistical analysis. The statistical analysis was performed using GraphPad Prism v6.0 (GraphPad, San Diego, California, USA). Data are represented as mean (SD). A calculated p-value of less than 0.05 was considered statistically significant. The biochemical (PicoGreen, Sircol, and DMMB) tests and gene expression assay were analyzed by two-way analysis of variance (ANOVA) with Sidak's multiple comparison post hoc test to compare the data timepoint of multi-layered scaffold with the corresponding timepoint of randomly aligned scaffold and to check

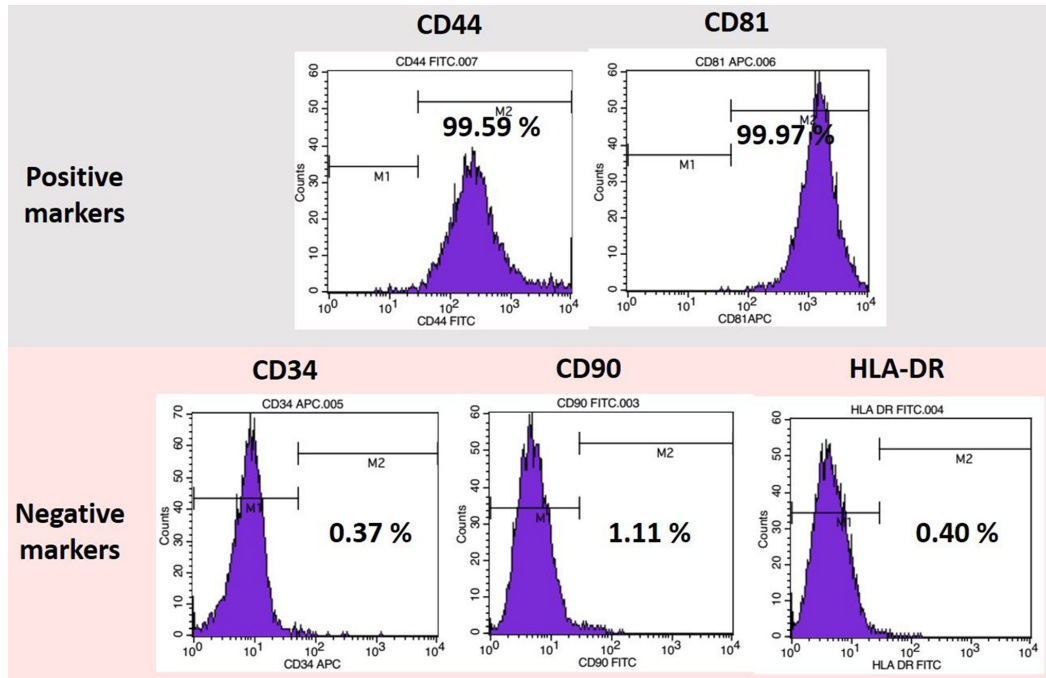


Fig. 1

Flow cytometry analysis showing the expression of mesenchymal stem cell (MSC) surface markers in rabbit bone marrow MSCs (BM-MSCs) ($n = 3$). The BM-MSC stained $> 99\%$ positive for CD44 and CD81 MSC surface markers and negative for CD34, CD90, and human leukocyte antigen - DR isotype (HLA-DR). APC, allophycocyanin; FITC, fluorescein isothiocyanate.

the significance between the two groups. In addition, for each scaffold the 28th day outcome was compared with the seventh day of its own to check the change in gene expression after differentiation. The statistical significance of histological scores, thickness of the cartilage, and percentage of collagen type 2 staining were calculated using one-way ANOVA with Tukey's multiple comparison test. The mean value and the significance between the groups was compared.

Results

Culture and characterization of rabbit MSCs. Rabbit bone marrow MSCs were cultured up to third passage. Flow cytometry analysis of the cells used for in vitro testing and transplant showed that they were more than 99% positive for CD81 and CD44 and less than 2% positive for the negative markers CD34, CD90, and HLA-DR (Figure 1). In vitro multilineage differentiation of MSCs showed their ability to become chondrocytes, osteoblasts, and adipocytes as demonstrated by deposition of GAG, calcium, and lipid droplets, respectively (Supplementary Figures aa, ab, ac).

In vitro testing of scaffolds. Cell distribution, viability, and proliferation on scaffold: confocal microscopic images taken in the sagittal plane showed that the cells were distributed in all three zones of the multi-layered scaffolds and throughout the randomly aligned scaffolds. Viability on cell-seeded scaffolds was evaluated using LIVE/DEAD assay. Both multi-layered and randomly aligned scaffolds showed higher numbers of viable cells with very few

dead cells as shown in Figures 2a and 2b. There was no difference in the percentage of live cells between the two scaffolds (Supplementary Figure a). We were unable to quantify the dead cell population due to the presence of genipin (a crosslinking agent used for the preparation of both scaffolds), which also has similar excitation-emission range as ethidium homodimer and exhibits red autofluorescence when viewed with a Texas Red filter. Further, to quantify the total DNA content on the cell-seeded construct, PicoGreen assay was performed. There was a significant increase in DNA content in the multi-layered scaffold during the course of differentiation compared to the randomly aligned scaffold. In the 28th day sample, the DNA content was 1.43-fold ($p \leq 0.005$, two-way ANOVA) higher in multi-layered scaffold, suggesting more cell proliferation in the multi-layered scaffold than in the randomly aligned scaffold (Figure 2c).

Histology and matrix synthesis: to visualize the GAG deposition on the scaffolds after four weeks of chondrogenic differentiation, Safranin O staining was performed. It was evident in multi-layered scaffolds that cells were aligned in the inter-fibre spaces and that secreted GAGs were orientated towards the fibres (Figure 3a). In addition, the cells were distributed throughout all three layers of the multi-layered scaffolds, whereas in the randomly aligned scaffolds the cells were more concentrated on the surface (Figure 3b). To further quantify the total GAG and collagen content, DMMB and Sircol assay were performed, respectively. On the 28th day, the mean GAG/DNA content was 597.3 ng in the multi-layered scaffold,

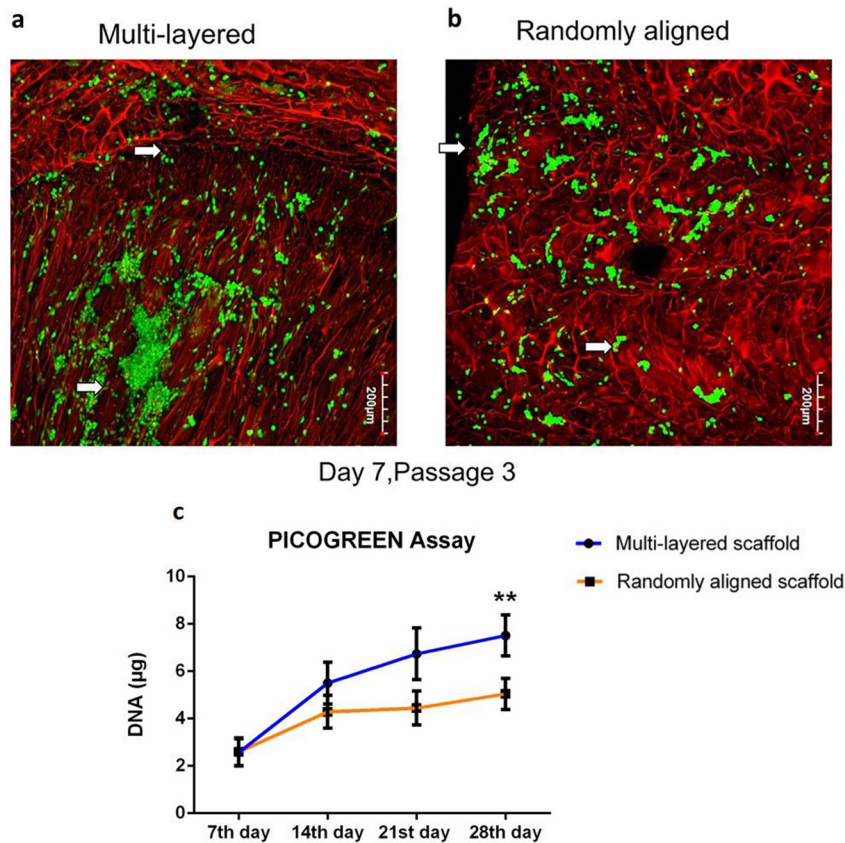


Fig. 2

A 3D reconstruction of confocal Z-stack images (10× magnification) representing LIVE/DEAD assay of rabbit bone marrow mesenchymal stem cells (BM-MSCs) cultured on a) multi-layered scaffold and b) randomly aligned scaffold. Green fluorescence indicates live cells and the white arrows pointing to red fluorescent dots indicate dead cells. Aligned fibres in the multi-layered scaffold are seen supporting more luxuriant growth of mesenchymal stem cells (MSCs) as compared to the randomly aligned fibres. The scaffold also demonstrates red auto-fluorescence, making it difficult to quantify dead cells (n = 3 independent experiments). c) Total DNA content per scaffold. **p = 0.005, two-way analysis of variance (ANOVA); after chondrogenic differentiation (28th day), significantly higher amounts of the total DNA were found in the multi-layered scaffold (blue line) compared to the randomly aligned scaffold.

which was significantly higher than that in the randomly aligned scaffold (427.5 ng; p = 0.007, two-way ANOVA) (Figure 3c). The total collagen content, quantitated using the Sircol assay, showed no significant difference between the two scaffolds (Figure 3d).

Gene expression analysis: the chondrocyte-specific marker (*COL2A1*), fibrocartilage marker (*COL1A1*), and chondrocyte hypertrophic marker (*COL10A1*) expressions were assessed by quantitative polymerase chain reaction (qPCR) assay. Gene expression analysis showed that *COL2A1* was significantly (p < 0.001, two-way ANOVA) increased between the seventh day and 28th day of chondrogenic differentiation on multi-layered (399 folds) and randomly aligned (349 folds) scaffolds (Figure 4a). When compared to the seventh-day sample, the expression of *COL10A1* and *COL1A1* was significantly (p < 0.001, two-way ANOVA) reduced in both types of scaffolds (Figures 4b and 4c). However, when compared between the two scaffolds, there was no significant difference. These outcomes indicate that both multi-layered and randomly aligned scaffolds support the chondrogenesis

of MSCs with significantly less fibrocartilage and hypertrophic cartilage formation.

In vivo testing of scaffolds. Gross appearance: at harvest, four months after treatment (in vivo group), untreated defects (Figure 5a) and defects treated with allogeneic chondrocytes (Figure 5b) were completely filled and regenerated with white tissue. The margin of the defects was well delineated in the allogeneic chondrocyte treated defects. The defects that were treated with scaffolds (both with and without cells) were completely filled with glossy white tissue that had integrated indiscernibly with surrounding AC (Figures 5c to 5f). Macroscopic observation did not show inflammation or loss of scaffold material. This outcome confirmed that the tested scaffolds were biocompatible.

Histological analysis. Safranin O staining was performed to assess the quality of cartilage regenerated in the defects. Repair of untreated AC defects was by thin fibrocartilage with a complete absence of Safranin O staining (Figures 5a' and 5a''). Defects treated with allogeneic chondrocytes regenerated with thick

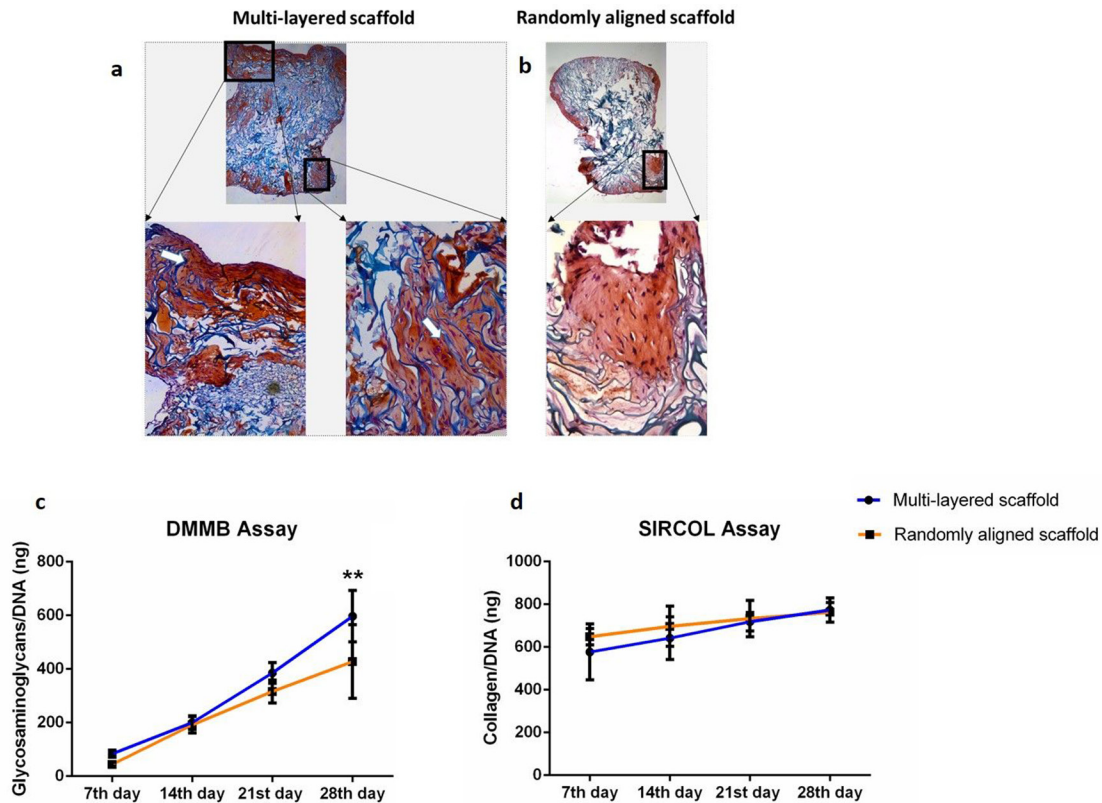


Fig. 3

Light microscopic representative images (first row: 4 \times ; second row: 10 \times magnification) demonstrate deep Safranin O staining of cell-seeded scaffolds after 28 days, indicating chondrogenic differentiation. The white arrows indicate the orientation of cells and glycosaminoglycan (GAG) along the fibres of the a) multi-layered scaffold, which is not found in the b) randomly aligned scaffold. Cell-seeded scaffolds during seven, 14, 21, and 28 days of chondrogenic differentiation showed significantly higher c) total GAG/DNA content on the 28th day in the multi-layered scaffold (blue line) compared to the randomly aligned scaffold. d) Total collagen/DNA content per scaffold did not show any significant difference between the two scaffolds ($n = 3$ independent experiments and each experiment was performed in duplicates). ** $p = 0.007$, two-way analysis of variance (ANOVA).

fibrocartilage accompanied by poor Safranin O staining (Figures 5b' and 5b''). Treated defects in both types of scaffold groups, either with or without cells, were stained profoundly with Safranin O, demonstrating good quality hyaline cartilage formation in the defects (Figures 5c' to 5f' and 5c'' to 5f''). The regenerated tissue in both types of scaffold groups had a smooth surface and integrated well with adjacent AC. In both types of scaffold groups, the subchondral bone thickness and trabecular bone volume underneath the regenerated cartilage were higher compared to the controls.

O'Driscoll score. The O'Driscoll scoring system was used to quantitatively evaluate the extent of cartilagenous repair. Defects treated with allogeneic chondrocytes and untreated defects had a low score with poor Safranin O staining, indicating poor quality regeneration. There was no significant difference in the groups that were treated with multi-layered scaffold with cells (mean 18.2 (SD 3.1)) and randomly aligned scaffold with cells (mean 18.5 (SD 2.1)). Similarly, there was no difference in the O'Driscoll score between the defects treated by multi-layered scaffold without cells (mean 17.7 (SD 1.9)) and

randomly aligned scaffold without cells (mean 17.1 (SD 3.75)) (Figure 5g).

When the scaffold treated defects were compared with the controls, the multi-layered scaffolds with cells exhibited a significantly higher score than the untreated defects (mean 13.4 (SD 3.2); $p = 0.003$, one-way ANOVA) and defects treated with allogeneic chondrocytes (mean 14.08 (SD 3.6); $p = 0.048$, one-way ANOVA). Similarly, the randomly aligned scaffold with cells scored significantly higher than the group 1 controls. The defects treated with multi-layered scaffolds without cells showed significantly higher regeneration than group 1 negative control, i.e. defects left untreated (Figure 5g). However, the randomly aligned scaffold without cells did not show any significant difference to group 1.

Immunohistochemistry. Of the two control groups, complete absence of staining was observed in untreated defects (Figure 6a), while defects treated with allogeneic chondrocytes exhibited patchy collagen type 2 staining (Figure 6b), confirming that the regenerated tissue was fibrocartilage. Control defects stained negatively for collagen type 10 (Figures 6a' and 6b'). Regenerated tissue in defects treated with multi-layered and randomly aligned

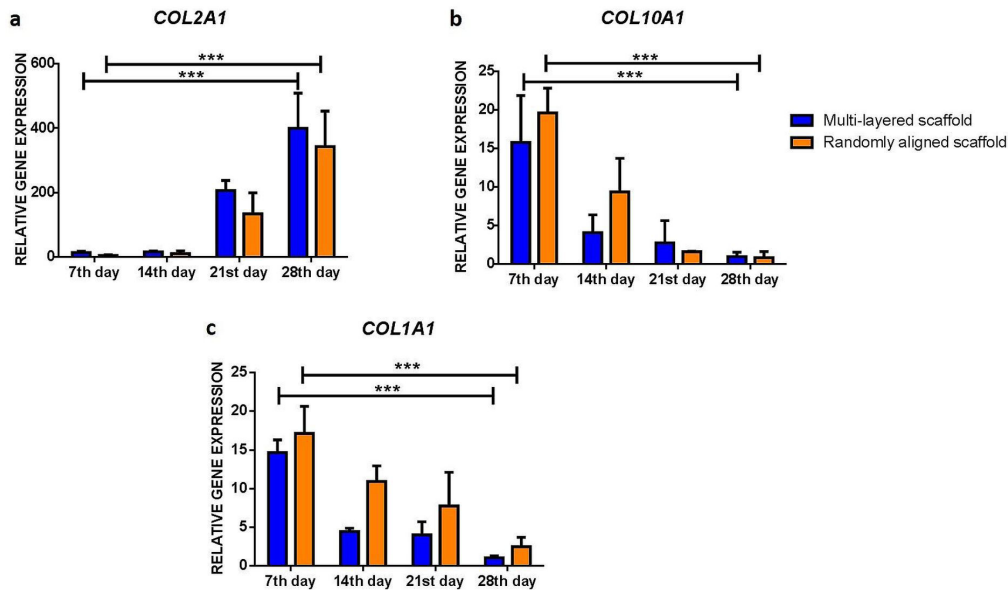


Fig. 4

Gene expression analysis on the cell-seeded scaffold during the in vitro chondrogenic differentiation showed good chondrogenesis in both the randomly aligned and multi-layered scaffolds. In the 28th day sample, *COL2A1* expression significantly increased ($p < 0.001$, two-way analysis of variance (ANOVA)) and *COL1A1* and *COL10A1* significantly decreased ($p < 0.001$, two-way ANOVA) compared to the seventh day sample. The comparison between the multi-layered and randomly aligned scaffolds did not show any significant difference. a) Cartilage-specific marker (*COL2A1*), b) hypertrophic chondrocyte marker (*COL10A1*), and c) fibrocartilage marker (*COL1A1*) ($n = 3$ independent experiments and each experiment was performed in duplicates). *** $p < 0.001$.

scaffolds (with and without cells) stained positively for collagen type 2, confirming that it was hyaline cartilage (Figures 6c' to 6f'). Regenerated tissue in the multi-layered and randomly aligned scaffold groups (with and without cells) stained negatively for collagen type 10, indicating absence of hypertrophic cartilage formation in the defects (Figures 6c' to 6f'). The percentage area of collagen type 2 staining was greater in the defects treated by the multi-layered scaffold loaded with cells (49.94%) than the randomly aligned scaffold with cells (29.10%; $p = 0.134$, one-way ANOVA), multi-layered scaffold without cells (22.39%; $p = 0.039$, one-way ANOVA), and randomly aligned scaffold without cells (19.54%; $p = 0.020$, one-way ANOVA) treated defects (Figure 6g). The comparison between the defects treated with two types of scaffolds without cells showed no significant difference. Taken together our results suggest that the quality of regenerated tissue was superior with cell-seeded multi-layered scaffolds, corroborating the results of Safranin O staining for GAG.

The mean thickness of regenerated cartilage as measured by the Safranin O stained layer was significantly ($p = 0.004$, one-way ANOVA) higher in multi-layered scaffolds with cells (574.72 μm (SD 160.93)) when compared to that in defects treated with randomly aligned scaffold with cells (354.99 μm (SD 91.44)). Similarly, the mean thickness of regenerated cartilage in multi-layered scaffold without cells treated defects (258.71 μm (SD 80.44)) was higher ($p = 0.644$, one-way ANOVA) compared to the randomly aligned scaffold without cells (189.36 μm

(SD 31.63)) group. In both the scaffold groups, scaffold loaded with cells showed significantly thicker cartilage formation compared to the scaffold without cells treated defects (Figure 6h). The control defects showed poor-to-zero Safranin O staining, so they could not be analyzed.

Discussion

The treatment of focal cartilage damage is vital as it unfailingly leads to osteoarthritis.¹⁸ The mechanical properties of AC are highly dependent on the density and composition of the ECM.¹⁹ Considering the complex chemistry, architecture, and mechanical properties of native cartilage, it is a challenge to design a biomimetic scaffold that facilitates mechanically superior AC regeneration.¹¹

We sought to test the importance of biomimetic structure in AC regeneration by using a multi-layered scaffold that closely mimics the structure of AC collagen matrix. These scaffolds facilitate tissue remodelling by providing a hydrophilic environment, native ECM conditions, and biodegradability. Further, they have already been characterized for their ability to absorb water, mechanical strength, and biocompatibility.¹¹ This study was specifically directed to test the ability of these scaffolds to induce in vitro and in vivo chondrogenesis using MSCs.

Soft scaffolds with a compressive modulus between 0.5 kPa to 4 kPa have been shown to support in vitro chondrogenesis of MSCs.¹⁶ The compressive modulus of multi-layered and randomly aligned scaffolds (2 kPa to 8 kPa) used in this study is in the ideal range for chondrogenesis

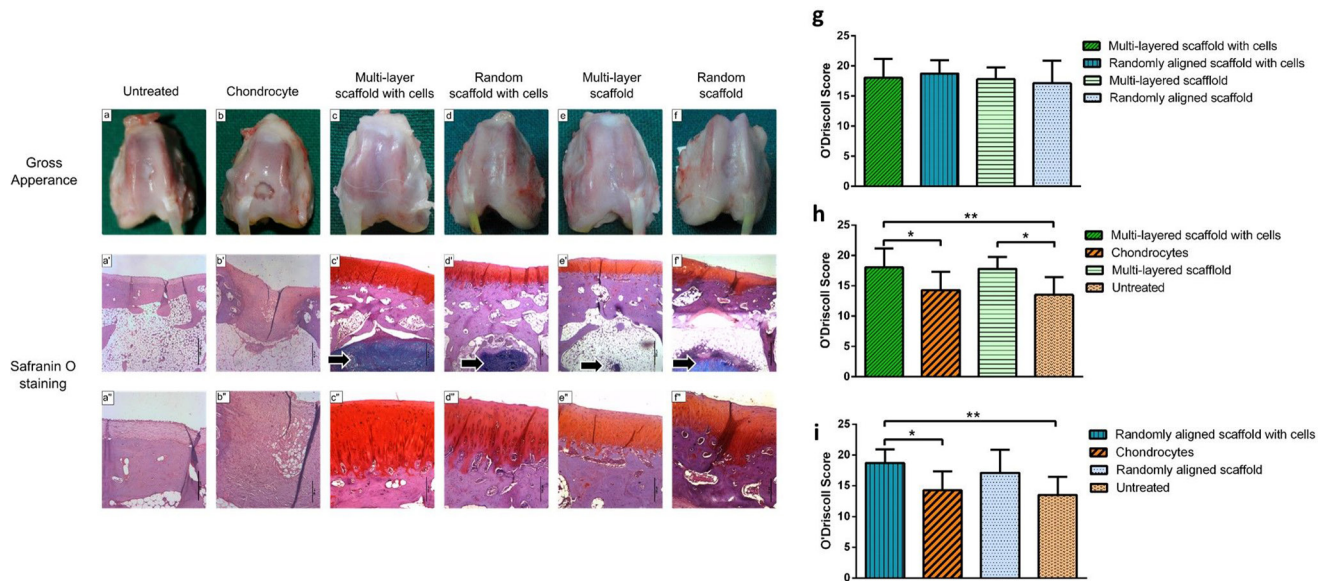


Fig. 5

Photographs representing the gross morphological appearance of harvested knees with regenerated articular cartilage defects in each group after four months' follow-up. Complete filling of the defect was observed in all groups including the untreated a) and b) chondrocyte-treated controls. However, the margin of defects was apparent in the chondrocyte-implanted defects. c) and d) The defects treated with both types of scaffolds with cells showed the best gross appearance compared to the e) and f) defects treated by scaffolds without cells. Light microscopic (middle row: 4× magnification, bar = 500 μm; lower row: 10× magnification, bar = 200 μm) images represent Safranin O staining of regenerated tissue in osteochondral defects. Defects treated with c') and c'') multi-layered scaffold with cells and d') and d'') randomly aligned scaffold with cells show more intense staining than those treated with scaffold without cells in the e') and e'') multi-layered and f') and f'') randomly aligned group. These show that both the scaffold with cell treated groups regenerated with good cartilage. Note the residual scaffold in scaffold treated defects (black arrow). The a') and a'') untreated and b') and b'') chondrocyte-treated controls show fibrocartilage repair with poor Safranin O staining. The bar charts represent the quantification of cartilage regeneration in treated and untreated defects. g) Multi-layered scaffold treatment compared with randomly aligned scaffold group showed no significant difference. h) Multi-layered scaffold treated defects (both with and without cells) showed higher O'Driscoll score than the controls (chondrocyte and untreated defect). i) Randomly aligned scaffold with cells exhibited significantly higher score compared with controls. O'Driscoll score confirmed that defects treated with both types of scaffolds exhibit high cartilage regeneration (scored more than 17) compared to the controls (score ≤ 14). *p < 0.05, one-way analysis of variance (ANOVA). **p < 0.01, one-way ANOVA.

of MSCs.^{16,20} A few studies have attempted to improve the compressive strength of CG scaffolds by glutaraldehyde crosslinking (260 kPa) and in situ precipitation (10.2 MPa).^{7,21} However, these may not be suitable for cartilage tissue engineering, as a scaffold with a compressive modulus of > 40 kPa favours bone formation.^{20,22}

CG scaffolds with either randomly aligned or multi-layered fibres were biocompatible and supported the growth of BM-MSCs. Moreover, the cells were distributed across all three zones in the multi-layered scaffold. This is in line with a previous report on aligned scaffolds using goat chondrocytes.¹¹ We observed that multi-layered scaffolds supported cell proliferation, as evidenced by a significantly higher DNA content than in scaffolds with randomly aligned fibres. The amount of ECM deposition in the tissue-engineered constructs is an indicator of good quality cartilage regeneration. In our study matrix deposition was significantly higher in multi-layered scaffolds than in randomly aligned scaffolds, but there was no difference in total collagen deposition. This is partly in line with a previously published study.²³ There are very few in vitro studies where multi-layered scaffolds have been tested.^{10,11,23,24} An in vitro study using goat infrapatellar fat pad MSCs on a multi-layered gelatin scaffold

showed good chondrogenesis with significantly higher collagen and GAG secretion (as demonstrated by Safranin O and biochemical assay) than that generated by a scaffold with randomly aligned fibres.²³ Another in vitro study on a multi-layered scaffold with polycaprolactone (PCL) showed significantly increased GAG expression and cell proliferation when compared to a non-aligned PCL scaffold.¹⁰

In this study, the influence of collagen fibril orientation on the in vitro tissue-engineered construct was studied by histology and gene expression. The qualitative observations in all six histology sections of multi-layered scaffold suggest that the orientation of cells and the secreted ECM were aligned in the direction of the scaffold fibres, while this was not seen in randomly aligned scaffold.

Several in vivo studies have used CG as a substrate for cartilage tissue engineering.²⁵⁻²⁷ In this study, the cartilage-specific marker collagen type 2 was significantly higher in both types of scaffold, indicating that CG favours chondrogenesis of MSCs irrespective of fibre alignment. There was a concomitant decrease in *COL1A1* and *COL10A1* expression in both the scaffolds, suggesting a decrease in fibrocartilage and hypertrophic cartilage formation. In our in vivo study, we found that both types

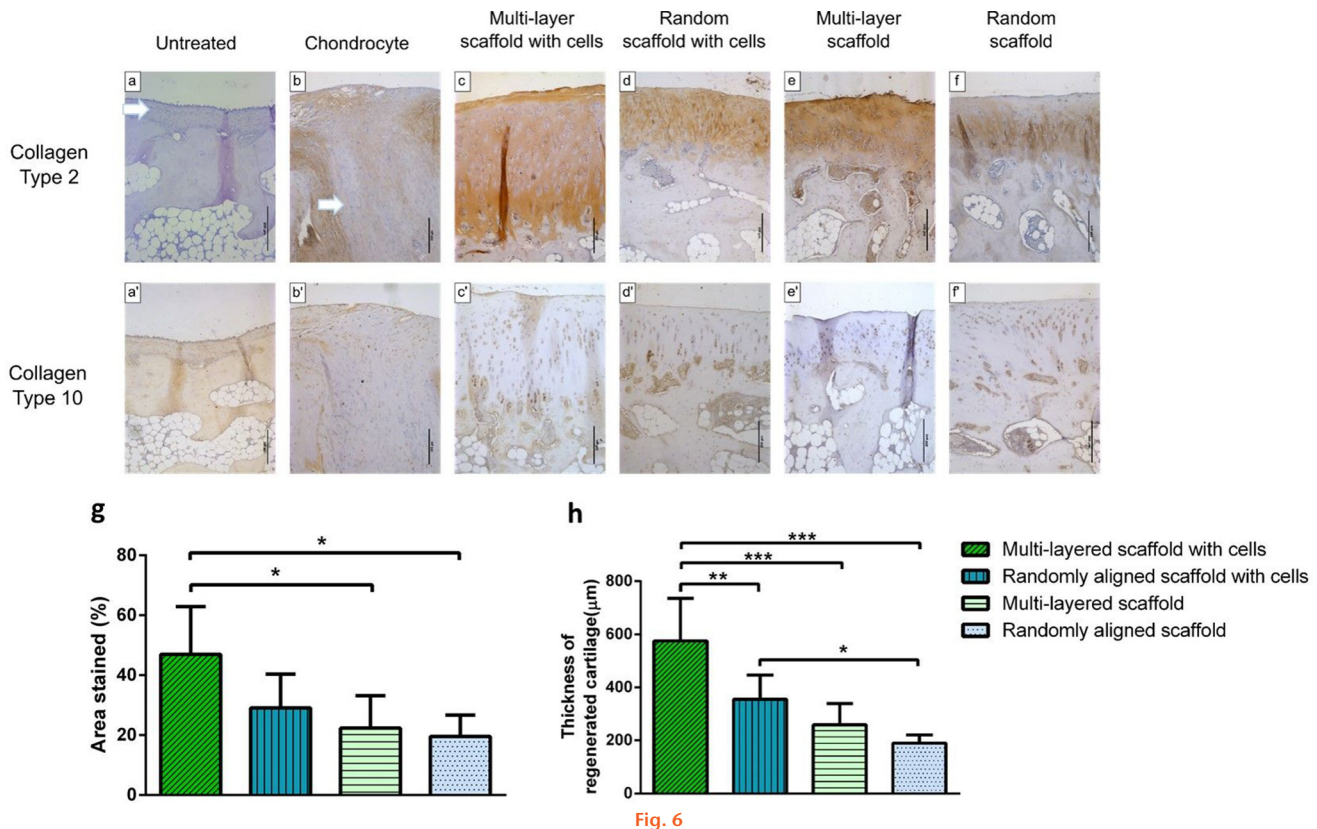


Fig. 6

Light microscopic images (10× magnification, bar = 200 μm) show collagen type 2 and collagen type 10 staining of regenerated tissue. The upper row shows collagen type 2 staining. In the control groups, a) untreated defects and b) defects treated with allogeneic chondrocytes were regenerated with fibrocartilage (white arrows indicate the absence of collagen type 2 staining). Brown colour indicates positive staining of collagen type 2, which confirms the hyaline cartilage formation in c) to f) both types of scaffold groups. Defects treated with c) multi-layered scaffold with cells and d) randomly aligned scaffold with cells showed the best staining with collagen type 2. In scaffold without cells treatment, defects treated with e) multi-layered scaffold showed better staining than the f) randomly aligned scaffold treated defects. The lower panel shows collagen type 10 staining. Its absence in a) and b) controls, c) and e) multi-layered scaffold groups, and d) and f) randomly aligned groups confirms the absence of cartilage hypertrophy in the regenerated tissue. The bar charts compare the quality of regenerated cartilage in test groups with and without cells. g) The percentage of collagen type 2 staining of regenerated cartilage in the multi-layered scaffold with cells was higher than that in other test groups. h) The thickness of articular cartilage was significantly higher in the defects repaired using scaffolds (multi-layer and randomly aligned) with cells compared to scaffolds without cells. Between multi-layer and randomly aligned, the multi-layered scaffold with cells showed significantly higher cartilage thickness. * $p < 0.05$. ** $p < 0.01$. *** $p < 0.001$. All p-values calculated using one-way analysis of variance (ANOVA).

of CG scaffolds did well when used with cells. It was interesting to further note that, even without cells, the multi-layered scaffold performed better than the untreated and allogeneic chondrocyte treated defects, suggesting that the inherent biomimetic arrangement of these fibres was more favourable for cartilage regeneration. Jia et al,²⁸ using a rabbit model, have shown that a vertically aligned scaffold produces better chondrogenesis than a randomly aligned scaffold in the short term; however, in the long term, there was no difference between the two. In vivo studies using multi-layered scaffolds have not been reported previously. Our study is the first to highlight the importance of biomimetic architecture in providing environmental cues for superior AC regeneration.

Studies have shown that osteochondral defects of a critical size either do not regenerate or result in fibrocartilage formation.^{29,30} In our study, we satisfactorily restored a patellar groove defect greater than critical size by using multi-layered and randomly aligned CG scaffolds. In the

control group, the gross appearance of well-demarcated margins with absence of Safranin O and collagen type 2 immunostaining indicates that untreated defects are bridged by inferior fibrocartilage. Surprisingly, allogeneic chondrocyte transplantation had a fair outcome. The use of cryopreserved chondrocytes that may have dedifferentiated during expansion could be a possible reason for a less favourable outcome (fibrocartilage formation) as observed in our case. Similar to our findings, other studies have also shown that culture-expanded allogeneic chondrocytes result in fibrocartilage formation with an O'Driscoll score similar to untreated defects.^{31,32} Defects treated using scaffolds with and without cells became filled with regenerated tissue that was indistinguishable from surrounding cartilage and displayed significantly higher O'Driscoll scores, presence of collagen type 2, and absence of collagen type 10 immunostaining, all of which demonstrate superior hyaline cartilage regeneration by CG scaffolds even without exogenous MSCs.

These outcomes in vivo, combined with a good in vitro profile, make the CG scaffold very suitable for human translation.

There were a number of limitations in this study. We did not track the cells in vivo to assess if the neocartilage was derived from the transplant or was of endogenous origin. Considering that scaffolds alone also performed well, it is possible that recruitment of native stem cells may have played a crucial role in the outcome. We avoided tracking as it causes additional stress to transplanted cells and might influence the outcome.³³

The age of the animal is a major contributor to the outcome, as spontaneous healing is said to occur in younger age groups.³⁴ In order to prove this point, although we have used adolescent rabbits (four months old) as reported in most of the studies, we attempted to create a defect of 4 mm in diameter in both treated as well as control defects, which is more than the critical size defect (3 mm).³⁵ Long-term follow-up of one year is more likely to extrapolate the results to humans, as short-term follow-up of four months in a rabbit model corresponds to three to four years of human life.³⁶

In conclusion, we tested the influence of biomimetic CG scaffolds with zonal architecture in regenerating osteochondral defects. We found that the tested scaffolds are well suited for AC tissue engineering. Although both multi-layered and randomly aligned scaffolds facilitated neocartilage formation in the defects, in vitro and in vivo studies demonstrated that the zonal arrangements influence chondrogenesis of MSCs and facilitated morphologically superior hyaline cartilage formation. The multi-layered scaffold alone, in the presence of endogenous stem cells, enabled hyaline cartilage regeneration in vivo and therefore can be considered as a standalone graft or impregnated with biomolecules to promote endogenous cartilage repair.

Supplementary material



Detailed descriptions of scaffold fabrication and multilineage differentiation, with corresponding figures along with representative histology images and a table showing the O'Driscoll scoring system used for the quantification of articular cartilage repair.

References

- Zhang L, Hu J, Athanasiou KA. The role of tissue engineering in articular cartilage repair and regeneration. *Crit Rev Biomed Eng*. 2009;37(1-2):1–57.
- Sophia Fox AJ, Bedi A, Rodeo SA. The basic science of articular cartilage: Structure, composition, and function. *Sports Health*. 2009;1(6):461–468.
- Knutsen G, Engebretsen L, Ludvigsen TC, et al. Autologous chondrocyte implantation compared with microfracture in the knee. A randomized trial. *J Bone Joint Surg Am*. 2004;86-A(3):455–464.
- Knutsen G, Drogset JO, Engebretsen L, et al. A randomized multicenter trial comparing autologous chondrocyte implantation with microfracture: long-term follow-up at 14 to 15 years. *J Bone Joint Surg Am*. 2016;98-A(16):1332–1339.
- Gobbi A, Nunag P, Malinowski K. Treatment of full thickness chondral lesions of the knee with microfracture in a group of athletes. *Knee Surg Sports Traumatol Arthrosc*. 2005;13(3):213–221.
- Li S, Sengers BG, Oreffo RO, Tare RS. Chondrogenic potential of human articular chondrocytes and skeletal stem cells: A comparative study. *J Biomater Appl*. 2015;29(6):824–836.
- Shen Z-S, Cui X, Hou R-X, et al. Tough biodegradable chitosan–gelatin hydrogels via in situ precipitation for potential cartilage tissue engineering. *RSC Adv*. 2015;5(69):55640–55647.
- Bhat S, Tripathi A, Kumar A. Supermacro porous chitosan-agarose-gelatin cryogels: in vitro characterization and in vivo assessment for cartilage tissue engineering. *J R Soc Interface*. 2011;8(57):540–554.
- Huang Y, Onyeri S, Siewe M, Moshfeghian A, Madhally SV. In vitro characterization of chitosan–gelatin scaffolds for tissue engineering. *Biomaterials*. 2005;26(36):7616–7627.
- McCullen SD, Autefage H, Callanan A, Gentleman E, Stevens MM. Anisotropic fibrous scaffolds for articular cartilage regeneration. *Tissue Eng Part A*. 2012;18(19-20):2073–2083.
- Arora A, Kothari A, Katti DS. Pore orientation mediated control of mechanical behavior of scaffolds and its application in cartilage-mimetic scaffold design. *J Mech Behav Biomed Mater*. 2015;51:169–183.
- Tan SL, Ahmad TS, Selvaratnam L, Kamarul T. Isolation, characterization and the multi-lineage differentiation potential of rabbit bone marrow-derived mesenchymal stem cells. *J Anat*. 2013;222(4):437–450.
- Lee TC, Lee TH, Huang YH, et al. Comparison of surface markers between human and rabbit mesenchymal stem cells. *PLoS One*. 2014;9(11):e111390.
- Khan IM, Gilbert SJ, Singhrao SK, Duance VC, Archer CW. Cartilage integration: evaluation of the reasons for failure of integration during cartilage repair. A review. *Eur Cell Mater*. 2008;16(16):26–39.
- O'Driscoll SW, Keeley FW, Salter RB. Durability of regenerated articular cartilage produced by free autogenous periosteal grafts in major full-thickness defects in joint surfaces under the influence of continuous passive motion. A follow-up report at one year. *J Bone Joint Surg Am*. 1988;70-A(4):595–606.
- Arora A, Kothari A, Katti DS. Pericellular plasma clot negates the influence of scaffold stiffness on chondrogenic differentiation. *Acta Biomater*. 2016;46:68–78.
- Gadjanski I, Yodmuang S, Spiller K, Bhumiratana S, Vunjak-Novakovic G. Supplementation of exogenous adenosine 5'-triphosphate enhances mechanical properties of 3D cell-agarose constructs for cartilage tissue engineering. *Tissue Eng Part A*. 2013;19(19-20):2188–2200.
- Randsborg PH, Brinchmann J, Løken S, et al. Focal cartilage defects in the knee - a randomized controlled trial comparing autologous chondrocyte implantation with arthroscopic debridement. *BMC Musculoskelet Disord*. 2016;17(1):117.
- Maldonado M, Nam J. The role of changes in extracellular matrix of cartilage in the presence of inflammation on the pathology of osteoarthritis. *Biomed Res Int*. 2013;2013:1–10.
- Foyt DA, Taheem DK, Ferreira SA, et al. Hypoxia impacts human MSC response to substrate stiffness during chondrogenic differentiation. *Acta Biomater*. 2019;89:73–83.
- Jiankang H, Dichen L, Yaxiong L, et al. Preparation of chitosan-gelatin hybrid scaffolds with well-organized microstructures for hepatic tissue engineering. *Acta Biomater*. 2009;5(1):453–461.
- Sun M, Chi G, Xu J, et al. Extracellular matrix stiffness controls osteogenic differentiation of mesenchymal stem cells mediated by integrin $\alpha 5$. *Stem Cell Res Ther*. 2018;9(1):52.
- Bhattacharjee A, Katti DS. Pore alignment in gelatin scaffolds enhances chondrogenic differentiation of infrapatellar fat pad derived mesenchymal stromal cells. *ACS Biomater Sci Eng*. 2018;5(1):114–125.
- Camarero-Espinosa S, Rothen-Rutishauser B, Weder C, Foster EJ. Directed cell growth in multi-zonal scaffolds for cartilage tissue engineering. *Biomaterials*. 2016;74:42–52.
- Diao H, Wang J, Shen C, et al. Improved cartilage regeneration utilizing mesenchymal stem cells in tgf- $\beta 1$ gene-activated scaffolds. *Tissue Eng Part A*. 2009;15(9):2687–2698.
- Whu SW, Hung KC, Hsieh KH, et al. In vitro and in vivo evaluation of chitosan–gelatin scaffolds for cartilage tissue engineering. *Materials Science and Engineering: C*. 2013;33(5):2855–2863.
- Chen J, Chen H, Li P, et al. Simultaneous regeneration of articular cartilage and subchondral bone in vivo using mscs induced by a spatially controlled gene delivery system in bilayered integrated scaffolds. *Biomaterials*. 2011;32(21):4793–4805.
- Jia S, Zhang T, Xiong Z, et al. In vivo evaluation of a novel oriented scaffold-bmsc construct for enhancing full-thickness articular cartilage repair in a rabbit model. *PLoS One*. 2015;10(12):e0145667.

29. Lv YM, Yu QS. Repair of articular osteochondral defects of the knee joint using a composite lamellar scaffold. *Bone Joint Res.* 2015;4(4):56–64.
30. Kazemi D, Shams Asenjan K, Dehdilani N, Parsa H. Canine articular cartilage regeneration using mesenchymal stem cells seeded on platelet rich fibrin: Macroscopic and histological assessments. *Bone Joint Res.* 2017;6(2):98–107.
31. Schreiber RE, Ilten-Kirby BM, Dunkelman NS, et al. Repair of osteochondral defects with allogeneic tissue engineered cartilage implants. *Clin Orthop Relat Res.* 1999;367(367 Suppl):S382–S395.
32. Katsube K, Ochi M, Uchio Y, et al. Repair of articular cartilage defects with cultured chondrocytes in atelocollagen gel. *Arch Orthop Trauma Surg.* 2000;120(3-4):121–127.
33. Ganini D, Leinisch F, Kumar A, et al. Fluorescent proteins such as eGFP lead to catalytic oxidative stress in cells. *Redox Biol.* 2017;12:462–468.
34. Ahern BJ, Parvizi J, Boston R, Schaer TP. Preclinical animal models in single site cartilage defect testing: a systematic review. *Osteoarthritis Cartilage.* 2009;17(6):705–713.
35. Cook JL, Hung CT, Kuroki K, et al. Animal models of cartilage repair. *Bone Joint Res.* 2014;3(4):89–94.
36. Dutta S, Sengupta P. Rabbits and men: relating their ages. *J Basic Clin Physiol Pharmacol.* 2018;29(5):427–435.

Author information:

- K. Rajagopal, PhD, Senior Research Fellow
- S. Ramesh, B.Tech, Senior Project Associate
- V. Madhuri, MS, MCh (Orth), Professor, Adjunct Scientist
Department of Paediatric Orthopaedics, Christian Medical College, Vellore, India;
Centre for Stem Cell Research (A Unit of inStem, Bengaluru), Christian Medical College, Vellore, India.
- N. M. Walter, MD (Path), Professor, Department of Forensic Medicine, Christian Medical College, Vellore, India.
- A. Arora, PhD, Senior Research Fellow
- D. S. Katti, PhD, Professor
Department of Biological Sciences & Bioengineering, Indian Institute of Technology Kanpur, Kanpur, India.

Author contributions:

- K. Rajagopal: Performed the in vitro and in vivo experiments, Drafted and reviewed the manuscript.
- S Ramesh: Provided technical assistance for the in vitro and in vivo experiments, Contributed to the first draft and reviewed the manuscript.
- N. M. Walter: Evaluated the histology, Reviewed the manuscript.
- A. Arora: Fabricated the scaffolds.
- D. S. Katti: Supervised and conceptualized the scaffold fabrication, Reviewed the manuscript, Acted as co-investigator for the project.
- V. Madhuri: Acted as the principal investigator for the project, Conceptualized, designed, and supervised the study, Performed the in vivo surgery and gross and tissue sectioning, Prepared and reviewed the manuscript.

Funding statement:

- This work was supported by the Science and Engineering Research Board (Grant number: SR/SO/HS-190/2012), Department of Science and Technology, Government of India. V. Madhuri reports personal support for travel to meetings and the provision of research equipment (to the Centre for Stem Cell Research, a Unit of InStem Bengaluru at Christian Medical College) from the Science and Engineering Research Board (SERB), related to this study. No benefits in any form have been received or will be received from a commercial party related directly or indirectly to the subject of this article.

ICMJE COI statement

- None declared.

Acknowledgements:

- We acknowledge Dr. Sanjay K.Chilbule and Dr. Bibhudutta Sahoo for the assistance provided during animal surgery.

Ethical review statement

- The study was approved by the institutional review board (IRB Min no:7403) and institutional animal ethics committee (13/2011), Christian Medical College, Vellore, India.

© 2020 Author(s) et al. This is an open-access article distributed under the terms of the Creative Commons Attribution Non-Commercial No Derivatives (CC BY-NC-ND 4.0) licence, which permits the copying and redistribution of the work only, and provided the original author and source are credited. See <https://creativecommons.org/licenses/by-nc-nd/4.0/>.